JOURNAL OF Materials CHEMISTRY

STM investigations of physisorbed monolayers of dialkoxy-substituted aromatics

Thomas Hansen,[a] Serge Itoua,[a] Fadhil S. Kamounah,[a] Jørn B. Christensen,[a] Thomas Bjørnholm,[a] Kjeld Schaumburg,[a] Klaus Bechgaard[b] and Stephen B. Wilkes[b]

[a]*Centre for Interdisciplinary Studies of Molecular Interactions, (CISMI), Dept. of Chemistry, University of Copenhagen, Symbion, Fruebjergvej 3, DK-2100 Copenhagen, Denmark. E-mail: K. Schaumburg@symbion.ki.ku.dk; fax: ⟨45⟩39271207; phone: ⟨45⟩35321821*
[b]*Risoe National Laboratory, Department for Materials Physics and Chemistry, DK-4000 Roskilde, Denmark*

Received 24th August 1998, Accepted 4th February 1999

The molecular adhesion layers studied in this work are comprised of symmetrical dialkoxy-substituted aromatics of the anthracene and biphenyl type, selected for their chemical and structural properties, *i.e.* 2,6-bis(octyloxy)anthracene, 2,6-bis(dodecyloxy)anthracene, 4,4′-bis(decyloxy)biphenyl and 4,4′-bis(hexadecyloxy)biphenyl. The characterization of these physisorbed monolayers is presented, and we propose plane-filling packing structure models for the 2D crystals. The models are based on sub Å calibrated images of the reproducibly scanned adhesion layers. The molecular 2D crystals formed yield domains of varying sizes.

1 Introduction

It has been known since the late eighties that certain organic molecules, like the liquid crystalline compound 4-octyl-4′-cyanobiphenyl (8CB)[1–3] and later didodecylbenzene (DDB, **1**), create physisorbed monolayers at the interface between a substrate, *e.g.* graphite, and solutions of the molecules in an organic solvent.[4] Also short oligomeric conjugated molecules have been successfully investigated for their self-assembling properties.[5] The liquid–solid interface constitutes what we call a nanophase, surrounded by bulk solvent on one side and the substrate on the other. The interest in this field arises from the expectation that it might find use in the new and rapidly growing field of nanotechnology, by using the ultrathin organic layers as functional elements.[6] Our aim in this study is to gain information on how molecules arrange in the nanophase and to study the effects of slight changes in positional substitution and alkyl chain length. We have chosen to study a series of C_2 symmetric anthracene molecules, suitably substituted with alkoxy groups. Anthracenes are well known for their ability to react in the 9,10 position in both cyclisation and electrophilic substitution reactions. For a regular packed monolayer of an anthracene derivative, we want to induce a dimerization reaction by a voltage pulse applied with the STM tip. This would lead to a contraction in the structure being clearly visible during the scanning. Similar polymerization experiments have been carried out with photoinduced reaction of diazoanthrone derivatives[7] and recently with diacetylenes.[8] We present STM images of two anthracene derivatives, 2,6-bis(dodecyloxy)-anthracene (**2**) and 2,6-bis(octyloxy)anthracene (**3**) at the interphase between highly oriented pyrolytic graphite (HOPG) and the high-boiling non-polar 1-phenyloctane.This paper will also present interfacial STM investigations of two alkoxy-substituted biphenyl compounds with varying alkyl chain lengths, 4,4′-bis(decyloxy)biphenyl (**4**) and 4,4′-bis(hexadecyl-oxy)biphenyl (**5**). We have selected two symmetric biphenyl derivatives because we wanted to study how the twist in the biphenyl moiety affects the 2D ordering of the molecules.

2 Experimental

2.1 Instrumentation

A Rasterscope 3000 scanning tunneling microscope from Danish Micro Engineering (DME),[9] working in constant current mode, was used in all cases to perform the STM measurements. As tip material we used a commercially available alloy Pt/Ir (90 : 10) wire. Tips were prepared by mechanical sharpening using a wire cutter of good quality. The tip quality was tested by scanning the (001) basal plane of a freshly cleaved piece of graphite at atomic resolution under ambient conditions. Only tips yielding a good image quality were used in further measurements. During all measurements the tip was biased negative relative to the graphite substrate.

2.2 Experimental procedure

A solution of the compound was prepared by dissolving 10–15 mg of powdered compound in 1 ml of a commercially available l-phenyloctane (bp 261–263 °C; purchased from Aldrich and used without further purification) by sonication for 5 min. A small droplet of this solution was deposited at ambient conditions on the (001) basal plane of a freshly cleaved piece of HOPG. The head of the STM apparatus is placed under a glass cover to protect the surface from dust and to decrease solvent evaporation during the experiment. By placing a small jar containing the solvent under the protective glass, the atmosphere will be saturated with l-phenyloctane vapor, further decreasing the evaporation rate of the solution droplet deposited on the HOPG. By this procedure we are able to prolong the existence of the physisorbed monolayer up to 48 h after surface deposition. The surface is then repeatedly rescanned through the liquid to obtain the atomic resolution of the graphite in order to check scanning/image quality. We noticed that the pictures of the graphite lattice we recorded scanning through the solution were often more contrasted than the images obtained when scanning through air. This we attribute to increasing coupling between the substrate and tip orbitals near the Fermi level.[10] When the droplet is deposited, the physisorption process of the molecules does not produce a monolayer immediately. It takes a certain time depending on the nature of the molecule scanned and the solution concentration. Subsequently we may begin to distinguish patterns on the surface, and after a fine adjustment of the scanning parameters, we can achieve images with a good contrast of the physisorbed, ordered monolayer (pSAM).

Calibration of the images was performed using the SPIP (scanning probe image processing) program version 3.0

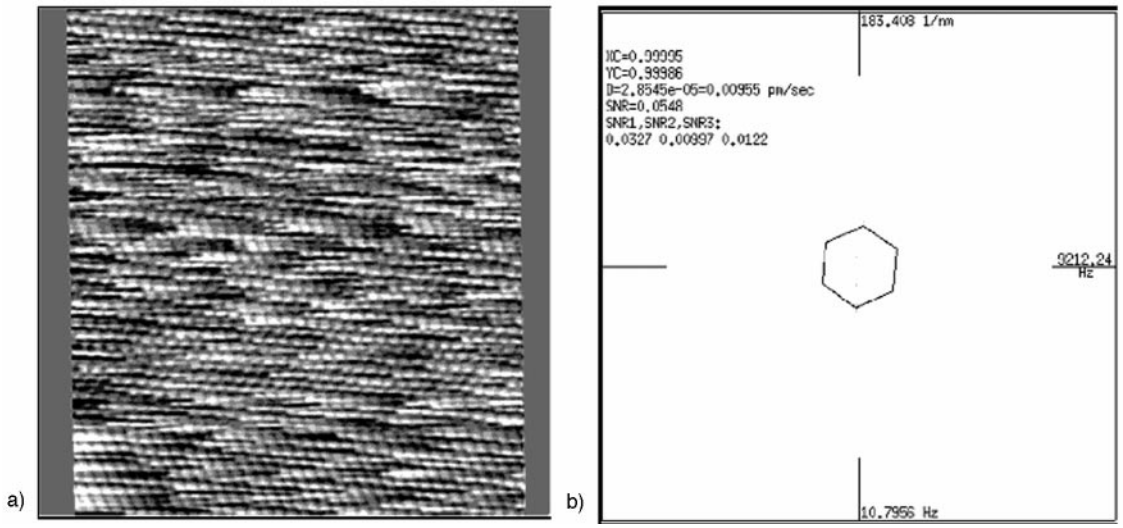

Fig. 1 Example of the calibration procedure. a) Calibrated HOPG image recorded under ambient conditions and calibrated in the scanning probe image program based on the unit cell dimension $\mathbf{a}=\mathbf{b}=0.246$ nm for the underlying hexagonal graphite. b) The Fourier transform of the graphite lattice.

(1996/97).[11] From the known dimensions of the graphite lattice parameters it is possible to calculate calibration factors for x, y, and drift—to obtain a calibrated HOPG image that deviates less than 0.01 Å from the one found *via* X-ray measurements. The calibration is based on the 2D Fourier spectrum of the crude image using a subpixel peak detection, developed for the program which has proven successful before.[12–14] Such a calibrated HOPG image is depicted in Fig. 1(a) (image 9×9 nm), with the 2D Fourier spectrum shown in Fig. 1(b). The corners of the hexagon are the directions of the six primary Fourier peaks of the spectrum. In Fig. 1(a) one can clearly see the atomic resolution—with each carbon atom site as a bright spot. The calibration factors from the HOPG image are conferred on the pSAM image recorded immediately thereafter.

3 Experimental results

All the following images are presented after calibration without any filtering process. All measurements and analyses of the STM images were carried out using the SPIP software. The images of the recorded HOPG lattice were used (for each compound) to calibrate the spatial measurements of the adhesion layers studied. Theoretical predictions of molecular dimension were made using a molecular modeling program, Spartan v. 4.0.[15] The dimension is defined as the distance between the two terminal alkyl hydrogen atoms in the molecule, optimized to a planar configuration.

2,6-Bis(dodecyloxy)anthracene (2)

Under our experimental conditions, the compound **2** generally formed the surface layer from the unsaturated solution ($10\ \mathrm{mg\ ml^{-1}}$) in less than 2 h. The compound showed formation of a stable monolayer of physisorbed molecules along one of the symmetry axes of the underlying HOPG. The images were recorded by scanning in constant current mode using a tunneling current $I=0.12$ nA and a bias voltage $V=$ 770 mV. These conditions allowed a good reproducible image. The scanning speed was 10 Hz ($10\ \mathrm{scanlines\ s^{-1}}$). This choice gave the best resolution possible. The image of the monolayer is shown in Fig. 2(a). Scanning on a smaller area ($8.8\times8.8\ \mathrm{nm^2}$, Fig. 2(b)), one can recognize the general structure for the adhesion layer. A series of images of the compound **2** allows us to suggest an interdigitated packing structure [Fig. 3(c)]. The **a** and **b** vectors of the pseudo unit cell[16] were found to be $\mathbf{a}=2.3$ nm and $\mathbf{b}=0.99$ nm and the smallest a–b angle γ is 61°, thus giving an area of the pseudo unit cell of $2.06\ \mathrm{nm^2}$. Computation yields a molecular length of 4.18 nm and 0.49 nm for the width to give a theoretical area $A_t=2.04\ \mathrm{nm^2}$.

Table 1 Structures of the investigated molecules

Molecule number	Molecule structure
1	$H_3C[H_2C]_{11}$–C$_6$H$_4$–$[CH_2]_{11}CH_3$
2	$H_3C(H_2C)_{11}O$–anthracene–$O(CH_2)_{11}CH_3$
3	$H_3C(H_2C)_7O$–anthracene–$O(CH_2)_7CH_3$
4	$H_3C[H_2C]_9O$–C$_6$H$_4$–C$_6$H$_4$–$O[CH_2]_9CH_3$
5	$H_3C[H_2C]_{15}O$–C$_6$H$_4$–C$_6$H$_4$–$O[CH_2]_{15}CH_3$

Table 2 Dimensions of the molecules together with measured and theoretical unit cell areas (determined using Spartan 4.0 from Wavefunction Inc.)

Molecule	L/ nm[a]	W/ nm[a]	**a**/ nm	**b**/ nm	γ/°	A (meas.)/ $\mathrm{nm^2}$	A (theo.)[a]/ $\mathrm{nm^2}$
2	4.18	4.88	2.38	0.99	61	2.07	2.04
3	3.16	4.88	1.70	1.20	79	2.01	1.54[b]
4	3.61	4.88	1.77	1.12	79	1.75	1.73
5	5.13	4.88	2.92	1.14	51	2.59	2.47

[a]Theoretical values determined by use of Spartan 4.0. [b]Remarkable difference between measured and calculated areas for **3**.

2,6-Bis(octyloxy)anthracene (3)

This molecule forms in less than 12 h a regular and stable physisorbed monolayer, that we can reproducibly image at a tunnel current of 0.1 nA and a bias voltage of 750 mV. As for compound **2** we kept a scanning speed of 10 Hz yielding

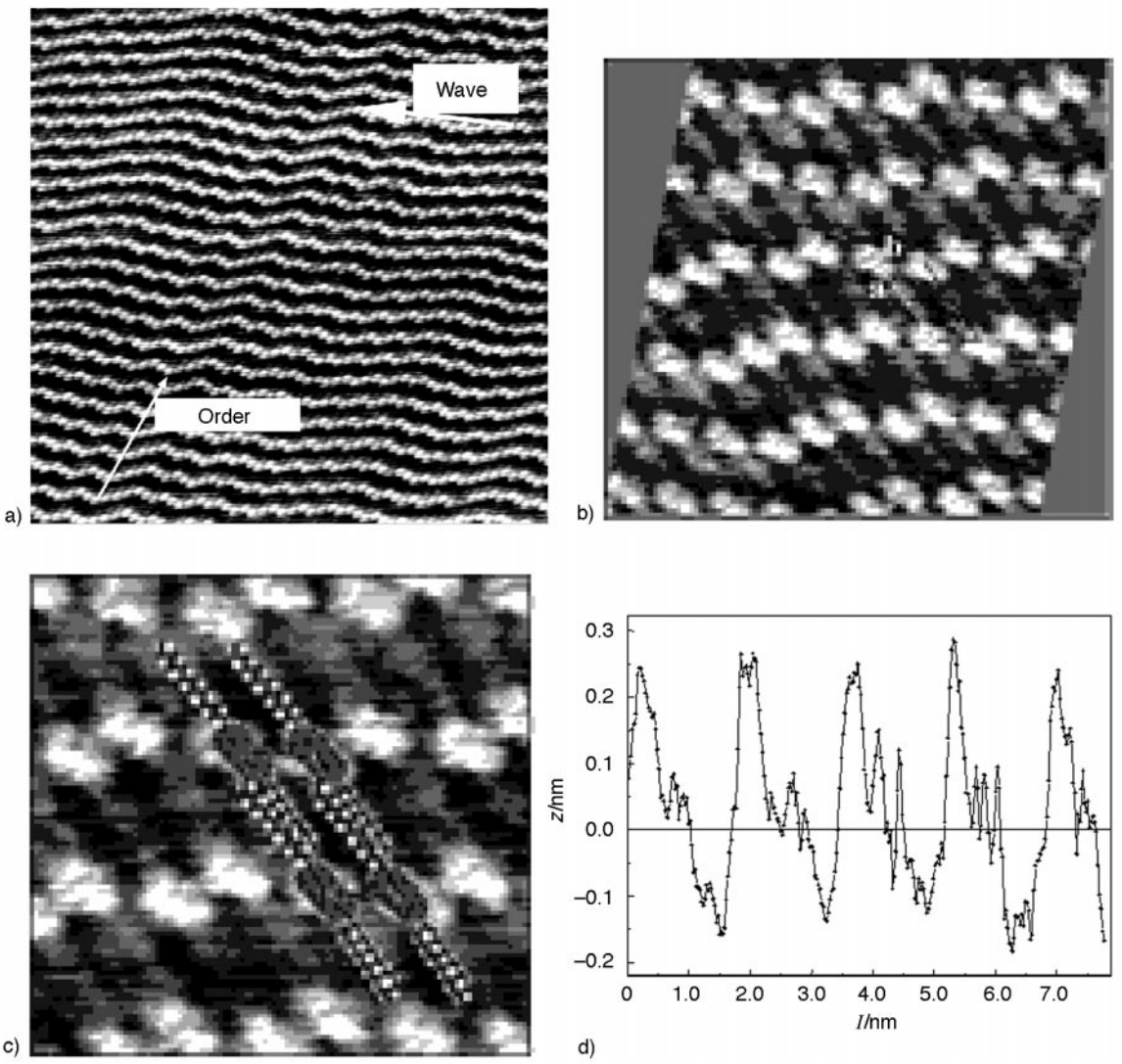

Fig. 2 STM images of 2,6-bis(dodecyloxy)anthracene **2**. Scan parameters: $V=710$ mV, $I=0.12$ nA, scanning speed 10 Hz. a) 50×50 nm^2 scan image with indications of the order–disorder phase; b) 9×9 nm^2 scan of the surface; and c) calibrated 9×11 nm^2 scan with the space filling model as superposition suggested in c. d) shows the heights profile along the path indicated by the white line in a).

reproducible images of the pSAM.The lattice vectors **a** and **b** for the calibrated image in Fig. 3(b) are $\mathbf{a}=1.69$ nm and $\mathbf{b}=1.20$ nm, and the *a*–*b* angle for the unit cell is $\gamma=79^\circ$. This yields a unit cell area of $A=1.99$ nm^2. Decreasing the scan size to 6×6 nm we can distinguish three different parallel segments per site, Fig. 3(b,c).

4,4′-Bis(decyloxy)biphenyl (4)

From a 15 mg ml^{-1} unsaturated solution, this compound formed a surface layer after about five hours of scanning under the above specified conditions. In Fig. 4(a) the pSAM appears stable and regular, without any domain formation or dislocations. The images were obtained using a bias voltage of 680 mV and a tunnel current of 0.12 nA which gave the best image contrast. Decreasing the scan size [Fig. 4(b) and (c)] to 9×9 nm afforded images with good submolecular resolution. We can distinguish some lines in the images representing the contrast from the alkyl chains. It appears from a careful analysis of the images recorded, that the alkyl side chains have two different orientations on the surface. The biphenyl moieties show a contrast appearing like an x at the surface under these specific scanning conditions. The appearance of the biphenyl moieties at each site seems to be quite diffuse. Varying the bias voltage did not change the contour or appearance of this aromatic moiety. Scanning smaller areas of the surface did not result in higher resolution. Although the biphenyl moiety of each molecule is still visible, the alkyl chains are poorly resolved no matter what scan parameters were chosen.

4,4′-Bis(hexadecyloxy)biphenyl (5)

This compound formed a surface layer after about six hours of scanning. Images were obtained showing a relatively stable and regular monolayer using a current of 0.10 nA and a bias voltage of 785 mV. These scanning parameters gave the best contrast throughout the investigation of this particular monolayer. When scanning on a large area [Fig. 5(a)] one observes a very regular adhesion layer, without any domain formation. From these calibrated images the unit cell dimension is determined to be $\mathbf{a}=2.38$ nm and $\mathbf{b}=1.14$ nm and the angle is $\gamma=73^\circ$ yielding a unit cell area of $A=2.595$ nm^2. Molecular modeling formed an optimized model with end to end molecular length of 5.12 nm and 0.49 nm for the width, yielding a theoretical unit cell area of $A_t=2.51$ nm^2.

Scanning a small area of the surface yields very good imaging of the surface, with resolution of both the biphenyl moiety and the side chain. Each biphenyl moiety gives a contrast appearing as four lines. These we attribute to the lowest unoccupied molecular orbitals (LUMO) in the molecule in analogy with Binning and others.[17] In Fig. 5(d) we have

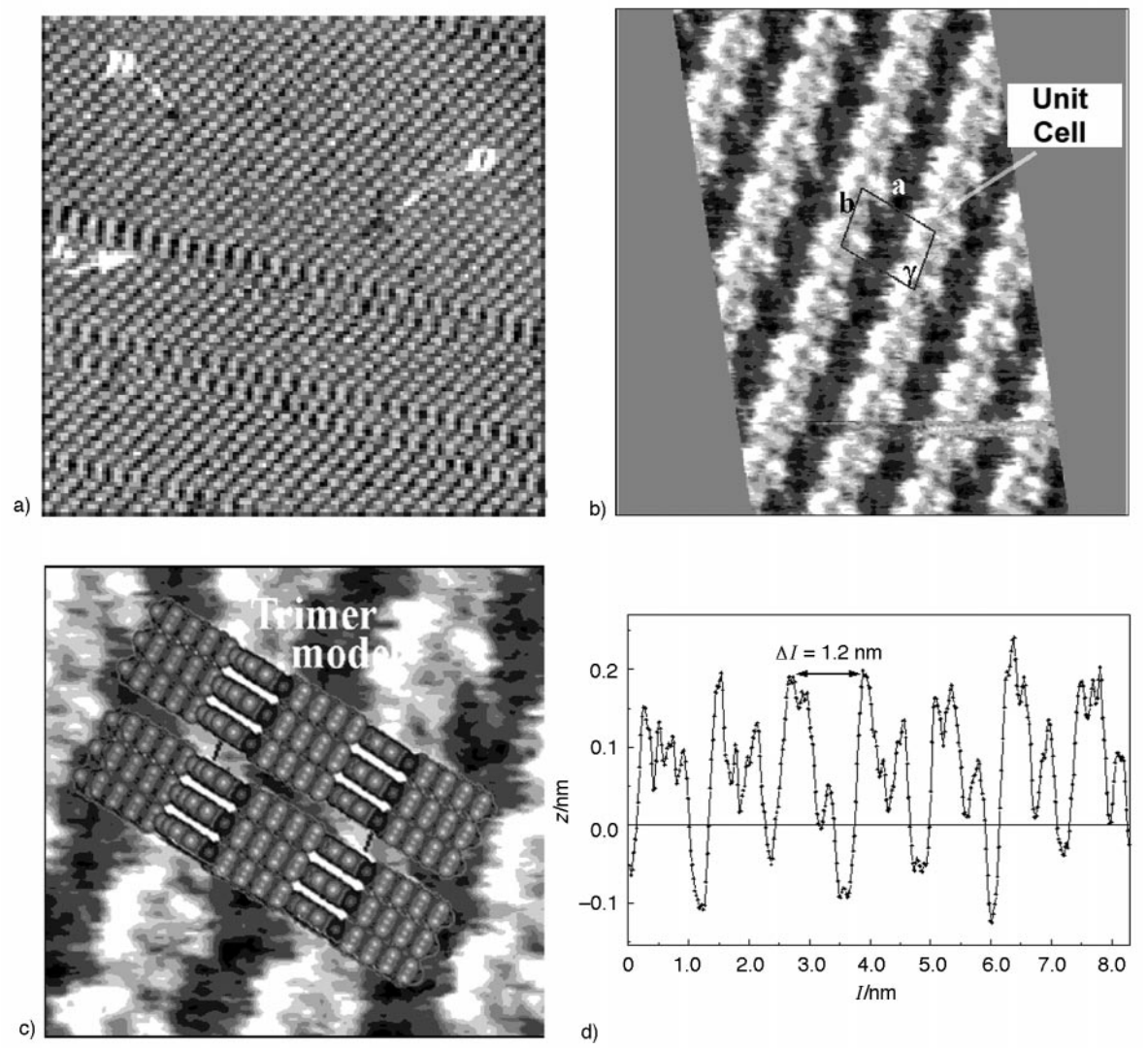

Fig. 3 STM pictures of 2,6-bis(octyloxy)anthracene **3**. Parameters: $V = 750$ mV, $I = 0.11$ nA, scanning speed 430 nm s^{-1} a) 30×30 nm^2 scanning view with domain formation; b) 9×9 nm^2 scan; c) 3×3 nm^2 scanning with superpositioned space filling molecular packing model; d) z-profile of molecules along **b** growth direction showing the variations in z over the sites.

made a cross section profile across two molecules parallel to the molecular length axis—from the cross section we can easily distinguish four peaks corresponding to each molecule. The molecular dimension is equal to the one found from Fourier transformations.

4 Discussion

From the study of the four anthracene based compounds it is our experience that the formation of a surface layer of these molecules takes the shortest time for derivative **2**, while we had to wait at least 12 h for the assembling of **3**. The dislocations in the monolayer of **2** along the indicated **b** growth direction is so far believed to be an intrinsic property of this compound under these specific conditions, thus, the anisotropic character of **2** yields a 1D order–disorder phase. This behavior has previously been reported by others,[18] *e.g.* for some chiral benzoate esters. To refine our interpretation of the measured data, we made a very simple approximation by viewing the molecule as a rectangular plane in space. Calculating the theoretical plane filling area per molecule as width × length of the rectangle gave a theoretical area A_t for **2** of 1.54 nm^2. Our results together with computer models lead us to suggest a packing model as depicted in Fig. 2(c) with one molecule in the pseudo unit cell. This compound is interesting because it forms an adhesion layer with inherent one-dimensionality.

The pSAM of the anthracene derivative **3** appears regular on the surface, with a nearly rectangular 2D unit cell, although defects and mismatch phenomena are noticed in the layer [Fig. 4(a)]. In the figure one notices missing sites (marked D) as well as the boundary at κ. We interpret this as molecules missing at the site during scanning due to diffusion to the bulk solvent.[9] To check the unit cell parameters using molecular modeling we structure-optimized the molecule in a planar geometry (π system and chain in the same plane—parallel to the surface). Using the same approximation as above we calculated the theoretical molecular area of **3** to $A_t = 1.54$ nm^2. This may be compared to the value from calibrated area measurement of 2.0 nm^2. The mismatch between the measured and calculated values for **3**, and the contrast in the images recorded, lead us to suggest the formation of a weak molecular trimer π-complex at the surface, with the aromatic plane of the molecules perpendicular to the surface. It is noteworthy that the contrast of this layer was different from **2** and it could not be explained by calculations of HOMO–LUMO levels in the molecules.

The two different biphenyl derivatives investigated in our work, **4** and **5**, both assemble into well ordered monomolecular layers. Compound **4** forms a uniform monolayer with large domains. Fig. 4(a) shows raw data for a 43×43 nm scan of the surface where the lamellas of molecules are clearly seen. One may notice alternating dark and bright shades forming a

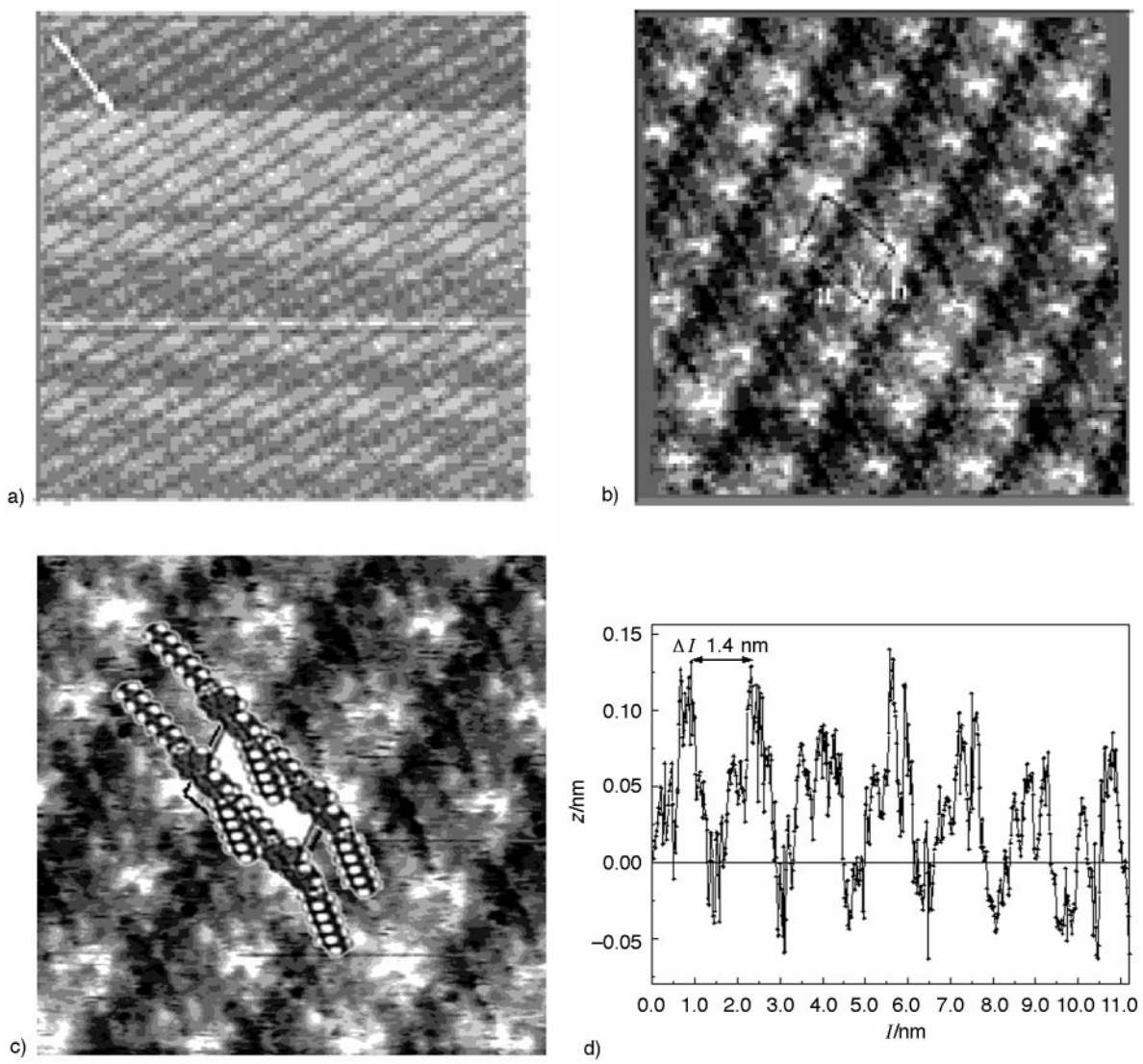

Fig. 4 STM pictures of the 4,4′-bis(decyloxy)biphenyl pSAM. Scanning parameters: $V = 680$ mV, $I = 0.12$ nA, scan speed 10 Hz. a) 43×43 nm^2 imaging without any indication of domain formation; b) 9×9 nm^2 surface scan with the unit cell drawn as an overlayer; c) space filling model suggested as a superposition on the original image; d) z-profile along the b direction, showing the corrugation of the adhesion layer over seven molecular sites.

superstructure in the monolayer. This superstructure is not a scanning artifact—we have determined its existence on several occasions in different scanning experiments, and the super lattice constant is the same when changing scan parameters and scan size. The super lattice forms a $1\mathbf{a} \times 3\mathbf{b}$ superstructure determined from visual image inspection. As shown in Fig. 4(b) and (c) the biphenyl moieties appear blurred. One can recognize a distinct orientation for the alkyl chains, and another weaker orientation of these chains 21° off the direction of the **a** vector. Based on the data determined and theoretical surface area for **4** we suggest a packing model as shown in Fig. 4(c) with one molecule in the unit cell.

On a 100 nm scan range, compound **5** forms a uniform monolayer. Domains of more than 100 nm size were recorded. Decreasing the scan length [Fig. 4(b)], we still recorded a well ordered molecular monolayer. On this scale one can see a $1\mathbf{a} \times 4\mathbf{b}$ superstructure in the monolayer as above for compound **4**. The presence of a superstructure for **4** and **5** can be explained by a model proposed by Rabe.[19] He suggests that the alkyl chain is oriented parallel or perpendicular to the surface in order to adapt to the graphite surface, thus leading to a slight difference in tunneling contrast. In Fig. 5(b) one can clearly distinguish the biphenyl moieties and the alkyl chain in the image. The molecules are arranged in an interdigitated packing, which we found to be very stable. The 2D crystal has a 2D oblique unit cell with measured area $A = 2.59$ nm^2. The biphenyl moieties are imaged as four slightly bent bright lines, with the conjugated system nearly parallel to the surface. These lines could be the contrast from tunneling to low-lying unoccupied states[11] in the molecule through a resonant tunneling mechanism.[20,21] This interpretation is in good agreement with our semi-empirical HOMO/LUMO calculations for this molecule. The alkyl chains are represented by a succession of spots parallel to the **b** vector in the unit cell. The chain under the specified scanning parameters in Fig. 5(b) gives a rather weak contrast. In Fig. 5(c) we propose a packing model based on the parameters acquired through scanning and a computer model of one molecule per unit cell in an interdigitated packing.

5 Conclusion

In the STM work we have studied the process of formation of physisorbed ordered monolayers of six aromatic molecules. Four of these produced stable two-dimensional crystals at the solvent–HOPG interphase. The 2,6-dialkoxyanthracene derivatives **2** and **3** formed layers where we could determine the dimensions with sub Å precision after calibration relative

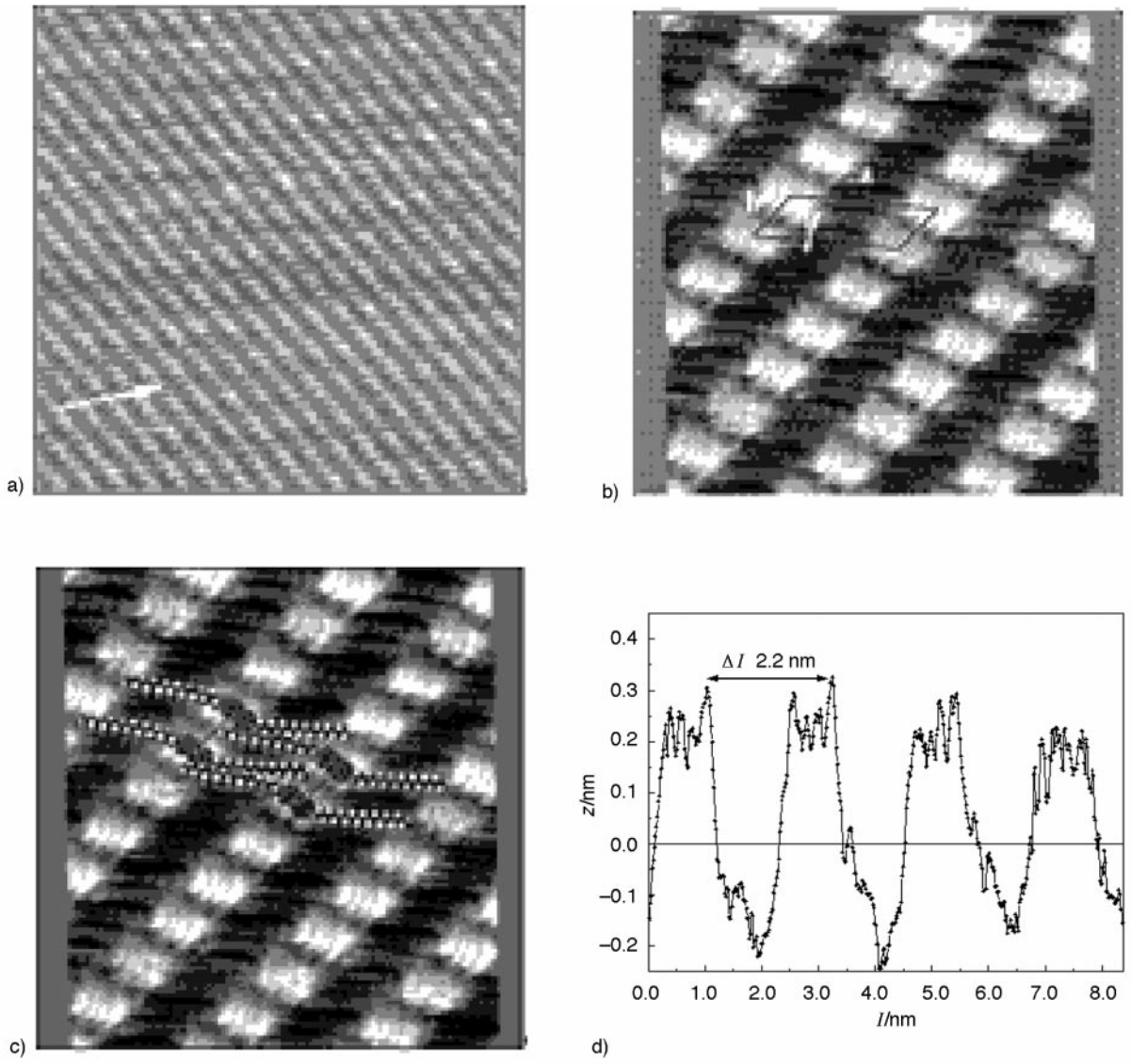

Fig. 5 STM images of 4,4′-bis(hexadecyloxy)biphenyl **5**. Parameters: $V = 785$ mV, $I = 0.10$ nA, scanning speed 10 Hz. a) Uncorrected 100×100 nm^2 scan without domain formation; b) 9×9 nm^2 scan with unit cell marked and with space filling packing model suggested in c); d) z contour curve over four sites along b showing the sites divided into four segments corresponding to the MOs of the molecule.

to known X-ray data for the graphite lattice. **2** formed an anisotropic order–disorder phase, while the derivative **3** formed a well ordered adhesion layer, which allowed us to study site and boundary defects. In the 4,4′-biphenyl compounds studied we were able to characterize the monolayer structure with sub Å precision. For **4** and **5** we detected the existence of a superstructure in the ordering of their 2D crystals. These results show that the alkyl chain length in the anthracenes has a pronounced influence on the stability and packing of the monolayer. Based on analysis of the Fourier spectra for the calibrated HOPG and the molecule images we find that all the studied pSAMs have a tendency to grow along the HOPG basal axis—except for compound **2**. Attempts to modify the 2D crystal of compound **2** by pulsing with the STM (5 V, 5 nm) had no measurable effect. For the biphenyl derivatives **4** and **5**, the monolayers formed are regular, with few domain formations. For compound **5** we achieved a very good image contrast with the specified measurement conditions—allowing us to resolve each aromatic ring in the molecule into two segments. The twist between the aromatic rings in the biphenyls did not seem to affect their ability to assemble. A model of each of the molecular 2D crystals is proposed and in each case, the calculated theoretical surface area per molecule A_t is in good agreement with the measured data except for compound **3**.

6 Synthesis

2,6-Bis(dodecyloxy)anthracene 2

Dodecanol 20 ml containing 3 ml of conc. HCl was added to a solution of 2,6-dihydroxyanthracene (1.0 g, 4.8 mmol) in 25 ml diethyl ether. The mixture was stirred at 60 °C for 16 h. Excess dodecanol was removed by vacuum distillation. The residue was subjected to silica gel eluting with CH_2Cl_2–*n*-hexane (1:1). The major yellow fraction was collected and the solvent removed *in vacuo* to obtain a pale yellow solid. Yield 0.40 g (15%); mp 135 °C. Elemental anal. ($C_{38}H_{58}O_2$): Calc. (%), C: 83.46; H: 10.69; found (%), C: 83.43; H: 10.57. ^{1}H NMR: ($CDCl_3$; δ) 0.80 (t, 6H), 1.20–1.30 (m, 32H), 1.50 (m, 4H), 1.80 (m, 4H), 4.00 (t, 4H), 7.00 (d, 2H), 7.05 (s, 2H), 7.75 (d, 2H), 8.10 (s, 2H). MS (EI): m/z 546 (M^+).

2,6-Bis(octyloxy)anthracene 3

This was prepared by a method similar to that described for compound **2** as a pale yellow solid, mp 159 °C. Elemental

anal. ($C_{30}H_{42}O_2$): Calc. (%), C: 82.96; H: 9.67, found (%), C: 82.92, H: 9.59. ^{1}H NMR: ($CDCl_3$; δ) 0.85 (t, 6H), 1.28–1.46 (m, 16H), 1.59 (m, 4H), 2.00 (m, 4H), 4.11 (t, 4H), 6.57 (s, 2H), 7.48 (m, 2H), 8.00 (m, 2H), 8.74 (s, 2H). MS (EI): m/z 434 (M^+).

4,4′-Bis(decyloxy)biphenyl 4

4,4′-Dihydroxybiphenyl (1.86 g, 10 mmol) and anhydrous potassium carbonate (6.61 g, 50 mmol) in 75 ml acetone containing 10% DMSO were heated for 30 min under argon. Whereupon 1-bromodecane (4.44 g, 20 mmol) in 10 ml dry acetone was added in one portion. The resulting mixture was heated for 12 h at reflux. The hot mixture was filtered and the solid was washed with hot acetone. The combined solvent was evaporated *in vacuo*. The white residue was redissolved in diethyl ether and washed with 1 M NaOH, then with water, and dried over anhydrous $MgSO_4$. The ether was removed *in vacuo* and the offwhite residue was recrystallized from dichloromethane to afford white lustrous plates. Yield 5.46 g (87%); mp 155 °C. Elemental anal. (C_{32} H_{50} O_2): Calc. (%), C: 82.34; H: 10.80; found (%), C: 82.26; H: 10.73. ^{1}H NMR: ($CDCl_3$; δ) 0.88 (t, 6H), 1.28 (m, 14H), 1.79 (m, 4H), 3.98 (t, 4H), 6.95 (dd, 4H), 7.44 (dd, 4H). MS (EI): m/z: 466 (M^+, 100%).

4,4′-Bis(hexadecyloxy)biphenyl 5

The synthesis was carried out using the procedure described for the preparation of compound **4** using 4,4′-dihydroxybiphenyl (1.86 g, 10 mmol), 1-bromohexadecane (6.11 g, 20 mmol), anhydrous potassium carbonate (6.61 g, 50 mmol) and dry acetone containing 10% DMSO (75 ml). The crude white solid isolated was recrystallized from dichloromethane to give white lustrous plates. Yield 7.62 g (90%); mp 119 °C. Elemental anal. ($C_{44}H_{74}O_2$): Calc. (%), C: 83.21; H: 11.75, found (%), C: 83.14, H: 11.69. ^{1}H NMR: ($CDCl_3$; δ) 0.88 (t, 6H), 1.27 (m, 26H), 1.79 (m, 4H), 3.98 (t, 4H), 6.96 (dd, 4H), 7.43 (dd, 4H). EI-MS: m/z 635 (M^+, 100%).

Acknowledgement

We wish to thank Dr Uwe Müller for providing the 2,6-bis(octyloxy)anthracene. We acknowledge financial support received from EU ESPRIT program 8523 PRONANO.

References

1 J. S. Forster and J. E. Frommer, *Nature* (*London*), 1988, **333**, 542; J. S. Forster, J. E. Frommer and P. C. Arnett, *Nature* (*London*), 1988, **331**, 324.
2 W. Mizutani, M. Shigeno, M. Ono and K. Kajimura, *Appl. Phys. Lett.*, 1989, **56**, 1974.
3 (*a*) D. L. Patrick and T. P. Beepe, Jr., *Langmuir*, 1994, **10**, 298; (*b*) F. Stevens, D. L. Patrick, V. J. Cee, T. J. Purcell and T. P. Beepe, Jr., *Langmuir*, 1998, **14**, 2396.
4 (*a*) M. Kimura, K. Sakurauchi, A. Okumura, K. Miyamura and Y. Gohshi, *Anal. Sci.*, 1991, **7**, 389; (*b*) R. Lazzaroni, A. Calderone, G. Lambin, J. P. Rabe and J. L. Brédas, *Synth. Met.*, 1991, **41–43**, 525; (*c*) G. C. McGornical, R. H. Bernhardt and D. J. Thomson, *Appl. Phys. Lett.*, 1990, **57**, 28.
5 F. Stevens, D. J. Dyer and D. M. Walba, *Langmuir*, 1996, **12**, 436.
6 T. Liu, J. P. Parakka, M. P. Cava and Y. T. Kim, *Synth. Met.*, 1995, **71**, 1989.
7 R. Heinz, A. Stabel, J. P. Rabe, G. Wegner, F. C. De Schryver, D. Corens, W. Dehaen and C. Süling, *Angew. Chem.*, 1994, **106**, 2154.
8 P. C. M. Grimm, S. De Feyter, A. Gesquiére, P. Vanoppen, M. Rücker, S. Valiyaveettil, G. Moessner, K. Müllen and F. C. De Schryver, *Angew. Chem., Int. Ed. Engl.*, 1997, **36**, 2601.
9 Danish Micro Engineering, Transformervej 12, DK-2730 Herlev, Denmark.
10 A. Stabel, P. Herwig, K. Müllen and J. P. Rabe, *Angew. Chem., Int. Ed. Engl.*, 1995, **34**, 1609.
11 J. F. Jørgensen, Scanning probe image restoration and analysis. PhD thesis, 1993, IMSOR, Technical University of Denmark, DK-2800 Lyngby. For additional information about the SPIP program and use thereof please contact J. F. Jørgensen at e-mail: JFJ@dfm.dtu.dk or the author.
12 J. F. Jørgensen, N. Schmeisser, J. Garnaes, L. L. Madsen, K. Schaumburg, L. Hansen and P. Sommer-Larsen, *Surf. Coat. Technol.*, 1994, **67**, 201.
13 J. Jørgensen, L. Madsen, J. Garnaes and K. Carniero, *J. Vac. Sci. Technol. B*, 1994, **12**, 1698.
14 L. Madsen, J. Jørgensen, K. Carniero, M. Jørgensen and J. Garnaes, *Synth. Met.*, 1993, **55**, 335.
15 Spartan program available from Wavefunction Inc., Irvine, CA 92715, USA.
16 Because of the one dimensionality of the order disorder phase a real 2D unit cell cannot be defined. We defined the pseudo unit cell as the one shown in Fig. 3(c).
17 D. P. E. Schmith, J. K. H. Hörber, G. Binning and H. Nejoh, *Nature* (*London*), 1990, **344**, 641.
18 D. C. Parks, N. A. Clark, D. M. Walba and P. D. Beale, *Phys. Rev. Lett.*, 1993, **70**, 607.
19 J. P. Rabe, *Ultramicroscopy*, 1992, **42–44**, 51.
20 D. M. Cyr, B. Venkataraman, G. M. Flynn, A. Black and G. M. Whitesides, *J. Phys. Chem.*, 1996, **100**, 13747.
21 A. Wawkuschewski, H. J. Cantow and S. N. Magonov, *Langmuir*, 1993, **9**, 2778.

Paper 8/06617E